Available online at www.sciencedirect.com
ScienceDirect
Journal of Environmental Sciences 2012, 24(3) 499–506
JOURNAL OF ENVIRONMENTAL SCIENCES
ISSN 1001-0742
CN 11-2629/X
www.jesc.ac.cn

Mn-CeO*x*/Ti-PILCs for selective catalytic reduction of NO with NH_3 at low temperature

Boxiong Shen*, Hongqing Ma, Yan Yao

College of Environmental Science and Engineering, Nankai University, 94 Weijin Road, Tianjin 300071, China

Received 28 February 2011; revised 25 April 2011; accepted 06 May 2011

Abstract

Titanium-pillared clays (Ti-PILCs) were obtained by different ways from $TiCl_4$, $Ti(OC_3H_7)_4$ and $TiOSO_4$, respectively. Mn-CeO_x/Ti-PILCs were then prepared and their activities of selective catalytic reduction (SCR) of NO with NH_3 at low-temperature were evaluated. Mn-CeO_x/Ti-PILCs were characterized by X-ray diffraction, N_2 adsorption, Fourier transform infrared spectroscopy, thermal analysis, temperature-programmed desorption of ammonia and H_2-temperature-programmed reduction. It was found that Ti-pillar tend to be helpful for the enlargement of surface area, pore volume, acidity and the enhancement of thermal stability for Mn-CeO_x/Ti-PILCs. Mn-CeO_x/Ti-PILCs catalysts were active for the SCR of NO. Among three resultant Mn-CeO_x/Ti-PILCs**,** the catalyst from $TiOSO_4$ showed the highest activity with 98% NO conversion at 220°C, it also exhibited good resistance to H_2O and SO_2 in flue gas. The catalyst from $TiCl_4$ exhibited the lowest activity due to the unsuccessful pillaring process.

Key words: Mn-CeO_x/Ti-PILCs; titania-pillared methods; low-temperature; SCR

DOI: 10.1016/S1001-0742(11)60756-0

Introduction

Selective catalytic reduction (SCR) of NO_x with NH_3 is an effective process for the cleaning of NO_x from stationary sources (García-Cortés et al., 2001). The catalysts based on V_2O_5-WO_3/TiO_2 are usually arranged upstream of air preheater performing high DeNO*x* activity at the temperature of 300–400°C. In order to avoid the deactivation by SO_2 and dust, SCR reactor is hoped to be located downstream of the particle control and the desulfurizer devices where the flue gas temperature is usually below 150°C. Therefore, it is needed to develop superior SCR catalysts at low temperature.

Among several metal oxides, Mn-CeO_x is believed to be a potential catalyst with high activity (Casapu et al., 2009; Qi et al., 2004) and high N_2 selectivity (Qi et al., 2004) in low-temperature SCR reaction. It yielded high NO conversion at 150°C but showed high vulnerability to sulfur poisoning (Qi et al., 2004). The activity or resistance to SO_2 poisoning can be enhanced by loading of catalysts on different supports such as TiO_2 (Li et al., 2007; Wu et al., 2008; Yu et al., 2010), active carbon (Tang et al., 2007), Al_2O_3 (Smirniotis et al., 2006) and ZSM (Carja et al., 2007). However, the use of all these supports is limited because of low resistance to sintering, low surface area or high cost.

Pillared interlayered clays (PILCs) are a kind of materials synthesized by exchanging the interlayered cations of smectites with bulky inorganic polyoxycations, followed by calcinations. Recently, pillared clays have been recognized as promising catalysts or catalytic supports for DeNO$_x$ processes in the temperature range (300–450°C) (Romero et al., 2006), based on the large surface area, unique porosity, thermal stability, acidity and reactivity. especially for Ti-PILCs, even Ti-PILC itself showed high activity as well as resistance to SO_2 and H_2O poisoning during SCR process of NO with NH_3 (Yang et al., 1992). Activities of Ti-PILCs in DeNO$_x$ process can be improved by their modification with different transition metals (e.g., Cu, Fe, V, Ce and Co) (Boudali et al., 2006; Chae et al., 2004; Chmielarz et al., 2003; Linda et al., 1996; Long and Yang, 1999, 2000; Yang and Li, 1995). Fe-exchanged Ti-PILC revealed better catalytic performance than the commercial V_2O_5-WO_3/TiO_2 even in the presence of H_2O and SO_2 at a temperature range of 300–400°C (Yang et al., 1992). Similar results have been found for V_2O_5/Ti-PILC (Boudali et al., 2006).

In spite of the confirmed ascendant catalytic properties of Ti-PILCs based catalysts in the SCR process at 300–400°C, to our knowledge, no previous paper dealing with the application of this relatively economic material to low-temperature SCR. These observations motivated us to combine Mn-CeO_x with Ti-PILCs to prepare Mn-CeO_x/Ti-PILCs and investigate their NH_3-SCR activity.

In this work, we studied some insight into some general properties and the activity of Mn-CeO_x/Ti-PILCs. Ti-PILCs were synthesized with different methods including

* Corresponding author. E-mail: shenbx@nankai.edu.cn

the novel method based on $TiOSO_4$ and two other general ways from $Ti(OC_3H_7)_4$ and $TiCl_4$ respectively.

1 Experimental

1.1 Catalyst preparation

The initial clay obtained from Tianjin Guangfu Fine Chemical Research Institute (China). CEC (83 meq/100 g) was used as a raw material for catalysts preparation without any physical or chemical pretreatment.

1.1.1 Ti-PILCs

To prepare the supports, three titanium pillaring agents were used to intercalate the natural clays. The first titanium pillaring agent was prepared by an addition of $TiCl_4$ into HCl solution (6.0 mol/L). The mixture was diluted with slow addition of distillated water for the final concentrations of Ti^{4+} and HCl reach 0.82 and 0.11 mol/L, respectively. The solution was then aged for 3 hr at room temperature. The second titanium pillaring agent from $Ti(OC_3H_7)_4$ was obtained by slowly adding the appropriate amount of $Ti(OC_3H_7)_4$ into a HCl solution (6.0 mol/L) under vigorous stirring. The final concentrations of titanium (0.25 mol/L) and HCl (1.0 mol/L) were obtained by adding water. The solution was aged for 3 hr prior to use. The third titanium pillaring agent was from $TiOSO_4$ using the method following literature (Binitha and Sugunan, 2006). $TiOSO_4$ (0.20 mol/L) was hydrolyzed by slow addition of $NH_3{\cdot}H_2O$ (10 wt.%,) until the reaction mixture attained a pH of 7.5. The precipitate obtained was separated, washed free of sulphate ions and further peptized by the addition of HNO_3 (10 wt.%) to get titania sol at pH of 1.6.

The suitable amounts of the obtained titanium pillaring agents, required to obtain the Ti/clay ratio of 15 mmol/g, were then added respectively to the vigorously stirred clay suspension which had been previously swelled for 24 hr. The clays were left in contact with the solution for 6 hr, then separated by filtration. The obtained materials were washed for several times to be free of Cl^-. Finally, the solids were dried at 110°C for 6 hr, calcined at 500°C for 3 hr and were denoted as Ti-PILC(Cl) (from $TiCl_4$), Ti-PILC(O) (from $Ti(OC_3H_7)_4$) and Ti-PILC(S) (from $TiOSO_4$), respectively.

1.1.2 Mn-CeO_x/Ti-PILCs

Supported Mn-CeO_x catalysts were prepared by an impregnation method with an mixed aqueous solution of $Mn(NO_3)_2$ and $Ce(NO_3)_3$. The final catalysts were obtained after dried at 85°C for 6 hr and calcined at 500°C for 5 hr. The loading of Mn (calculated as Mn_2O_3) and Ce (calculated as CeO_2) was 12 wt.% in total with a weight ratio of Mn_2O_3/CeO_2 = 1:1.

1.2 Catalyst characterization

Textural properties of the samples were measured by N_2 adsorption/desorption at liquid nitrogen temperature using a NOVA 2000 automated gas sorption system (Quantachrome Instruments, USA), the samples were degassed under vacuum at 200°C for 2 hr before the measurements. The powder X-ray diffraction (XRD) patterns were recorded on Rigaku 2500 system using Cu $K\alpha$ radiation (40 kV, 100 mA) (Rigaku Corporation, Japan). Thermo gravimetric (TG) and Differential scanning calorimeter (DSC) analyses were performed on 0.01 g of sample under a nitrogen flow of 20 mL/min using a heating rate of 10°C/min from room temperature to 1000°C (METSH Apparatus, Germany). Fourier transform infrared spectroscopy (FT-IR) spectra were recorded on a Nicolet Magna-560 infrared spectrometer (Thermo Nicolet Corporation, USA), the catalysts were pressured into self-supporting wafers and placed in a high-temperature cell with KBr window, a total of 100 co-added scans with a spectral resolution of 4 cm^{-1} were collected over the spectral range 4000–400 cm^{-1}. The temperature programmed desorption (NH_3-TPD) and temperature programmed reduction (H_2-TPR) experiments were performed on tp-5080 automated chemisorption analyzer (Tianjin Xianquan Instrument, China) using 0.1 g catalysts. For NH_3-TPD experiments, after a pretreatment in pure N_2 at 500°C for 0.5 hr, the catalysts were cooled down to room temperature in pure N_2 and then saturated for 0.5 hr with a stream of pure NH_3 (total flow rate = 30 mL/min). After saturation, the catalysts were flushed in a pure N_2 flow for 0.5 hr at 100°C. Finally, the TPD of NH_3 was carried out in pure N_2 at a heating rate of 10°C/min from 100 to 500°C. Prior to H_2-TPR experiments, the samples were firstly pretreated in pure N_2 at 500°C for 0.5 hr, and then cooled down to room temperature. TPR runs were carried out in a flow of H_2 (5 vol.%) in N_2 (30 mL/min) from room temperature to 650°C with a heating rate of 10°C/min. The NH_3 desorption (or H_2 uptake) was measured quantitatively by a thermal conductivity detector (TCD).

1.3 Catalytic activity test

The SCR activity of the catalysts for NO removal with NH_3 was carried out in a fixed-bed flow reactor. Four gas streams, 0.06 vol.% NO, 0.06 vol.% NH_3, 3 vol.% O_2, 3 vol.% H_2O (when used), 0.01 vol.% SO_2 (when used) and pure N_2 in balance were used to simulate the flue gas. In all the runs, the total gas flow rate was maintained at 300 mL/min over 0.5 g catalyst (40–60 mesh). The feed gases were mixed and preheated in a chamber before entering the reactor. During the measurements, the concentrations of NO at the inlet and outlet of the reactor were monitored by Flue Gas Analyzer (KM900, Kane International Ltd., UK) equipped with NO sensor. The activities of the catalysts were measured by the conversion of NO calculated as follows:

$$R = \frac{C_{in} - C_{out}}{C_{in}} \times 100\%$$

where, R is NO conversion, C_{in} and C_{out} are the NO concentration at the inlet and outlet of the fixed-bed flow reactor.

2 Results and discussion

2.1 Characterization

2.1.1 N_2 adsorption/desorption results

Compared to Mn-CeO_x/clay, Mn-CeO_x/Ti-PILCs preserved a larger surface area and pore volume, while a smaller average pore diameter (Table 1). Among all three Mn-CeO_x/Ti-PILCs, Mn-CeO_x/Ti-PILC(O) and Mn-CeO_x/Ti-PILC(S) exhibited the largest surface areas and pore volumes respectively, while Mn-CeO_x/Ti-PILC(Cl) possessed the smallest surface area and total pore volume.

Table 1 Physical properties of the samples

Samples	BET specific surface area (m^2/g)	Total pore volume (cm^3/g)	Average pore diameter (nm)
Mn-CeO_x/clay	45.35	0.08062	7.111
Mn-CeO_x/Ti-PILC(Cl)	81.45	0.1163	5.710
Mn-CeO_x/Ti-PILC(O)	133.7	0.1320	3.958
Mn-CeO_x/Ti-PILC(S)	117.0	0.1420	4.877

N_2 adsorption/desorption isotherms and pore distributions of the supported Mn-CeO_x catalysts are presented in Fig. 1. All the adsorption isotherms and hysteresis loops of the samples seemed to be of type IV and type H3 according to IUPAC classification (Gregg and Sing, 1982). In all isotherms, the desorption branch showed an obvious inflection "knee" at about P/P_0 of 0.40–0.50, which has been observed for many different types of layered materials when nitrogen was used as the adsorbent (nitrogen boils at P/P_0 0.42) (Auerbach et al., 2004; Cool et al., 2004; Yuan et al., 2006). A narrow distribution of mesopores with a diameter of about 2.7–5.0 nm was observed for all the catalysts (Fig. 1b).

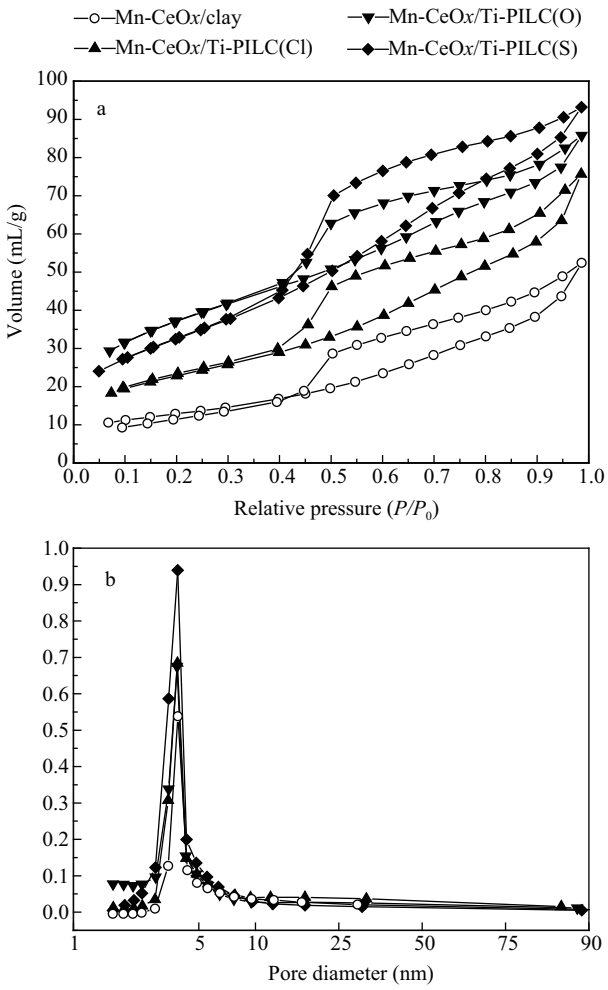

Fig. 1 N_2 isotherms adsorption/desorption (a) and pore size distribution of the catalysts (b).

2.1.2 XRD results

Since the samples used were randomly oriented powder, the X-ray powder diffraction patterns showing the basal (001) reflection was considered as one of the main identification sources for the clay groups. As illustrated in Fig. 2, the initial clay showed a main peak at approximately 2θ of 9°, which was commonly assigned to the basal (001) reflection.

For all the three Mn-CeO_x/Ti-PILCs, a broad and flat peak spanning over 25–27° was due to inserted TiO_2 which related to the pillaring process that the entrance of titanium pillar replaced some exchangeable cations. The XRD patterns of Mn-CeO_x/clay retained the characteristic (001) diffraction which was also found for Mn-CeO_x/Ti-PILC(Cl) but absolutely absent in Mn-CeO_x/Ti-PILC(O). For Mn-CeO_x/Ti-PILC(S), a diffuse and ill-defined (001) diffraction peak was found. It was considered that the effective pillaring of titania might cause the absence of (001) diffraction peak (Sing et al., 1985), which was probably correlated with a delamination process of the clays (Yang et al., 1992). During the delamination process, the long range face-to-face association was no longer present, and the material was characterized by the non-parallel ordering of aluminosilicate layers. Accordingly, it might be deduced that the disappearance of (001) diffraction peak for Mn-CeO_x/Ti-PILC(O) was ascribed to the successful pillaring process of titania; while Mn-CeO_x/Ti-PILC(Cl) was not well pillared. For Mn-CeO_x/Ti-PILC(S), the profile of (001) peak might be due to non-uniform pillaring of the clay layers in resultant Ti-PILC(S). On the other hand, for Mn-CeO_x/Ti-PILC(S), it was noteworthy that the peak

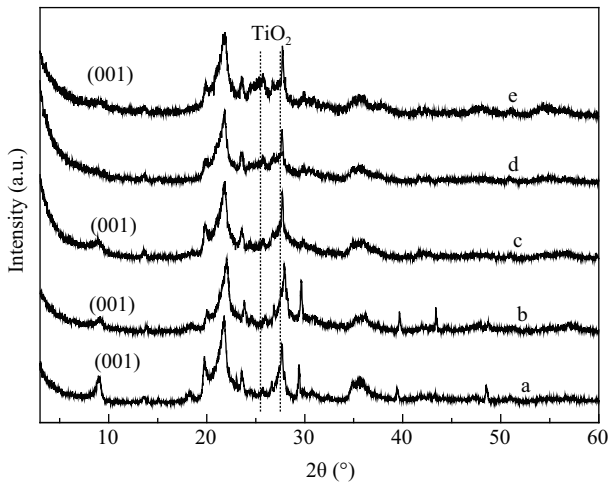

Fig. 2 XRD patterns of the materials. Line a: clay; line b: Mn-CeO_x/clay; line c: Mn-CeO_x/Ti-PILC(Cl); line d: Mn-CeO_x/Ti-PILC(O); line e: Mn-CeO_x/Ti-PILC(S).

at about 25.3° which could be attributed to the (101) reflection of anatase TiO_2, was much more intense than the other two Mn-CeO_x/Ti-PILCs. It indicated the presence of extra-lattice TiO_2 for Mn-CeO_x/Ti-PILC(S) (Yang et al., 1992).

Consistent with many supported manganese and cerium mixed oxides, there were no peaks for MnO_x or CeO_x in the XRD patterns of all the Mn-CeO_x/Ti-PILCs, the absence of manganese or cerium oxide phases could be attributed to a high dispersion and/or low crystalline nature of metal oxides in these samples.

2.1.3 TG results

The TG and DSC curves for samples including Mn-CeO_x/clay and Mn-CeO_x/Ti-PILCs are shown in Fig. 3. Before the TG and DSC experiments, all the samples were calcined at 500°C for 5 hr during the catalysts preparation. In the TG experiments, the main weight losses occurred in three steps, at 25–150°C, 200–550°C and 600–725°C. The first step corresponded to the loss of physically adsorbed water. It was hard to attribute the following two steps respectively. They were assumed mainly related with dehydroxylation of structural hydroxyl groups resulted from either the dehydroxylation of the clay structure, or removal of any remaining hydroxide from Ti-PILCs (Binitha and Sugunan, 2006). Mn-CeO_x/clay showed a higher weight loss than Mn-CeO_x/Ti-PILCs, especially in the third steps. Among the three Mn-CeO_x/Ti-PILCs, Mn-CeO_x/Ti-PILC(Cl) suffered a larger weight loss compared to Mn-CeO_x/Ti-PILC(O) and Mn-CeO_x/Ti-PILC(S).

In the DSC curves of Mn-CeO_x/clay, three endothermic peaks concerning dehydroxylation of structural hydroxyl groups or even collapse of the structure was were visible around 350, 540, and 700°C. The endothermic peak at 910°C should be attributed to the formation of cristobalite resulting from calcination on the Mn-CeO_x/clay. For Mn-CeO_x/Ti-PILCs, there were much more obvious exothermic characters because of more structural hydroxyl introduced with Ti-pillaring effect. Among all three Mn-CeO_x/Ti-PILCs, the endothermic peak located at 650°C which was much higher than that of Mn-CeO_x/clay, could be assigned to probable collapse of the structure, it further revealed the unsuccessful pillaring process which were also supported by the relatively larger weight loss. It was noteworthy that Mn-CeO_x/Ti-PILC(S) showed most significant exothermic peak which might also be comprehended on the basis of influence of its more extra-lattice TiO_2.

Combing the weight loss of Mn-CeO_x/Ti-PILCs (Fig. 3A) and endothermic peaks of the samples (Fig. 3B), it confirmed that Ti-pillar can enhance the thermal stability of Mn-CeO_x/Ti-PILCs. The thermal stability order is as follows: Mn-CeO_x/T-PILC(S) > Mn-CeO_x/Ti-PILC(O) > Mn-CeO_x/Ti-PILC(Cl) > Mn-CeO_x/clay.

2.1.4 NH_3-TPD results

Figure 4 illuminates NH_3-TPD runs performed over Mn-CeO_x/Ti-PILCs and Mn-CeO_x/clay. In all the cases, the spectra showed similar features with a broad shape spanning in the wide temperature range from 100 to 500°C, which evidenced with the presence of several NH_3 species with different thermal stability on the surface of the catalysts. Note that the desorption peaks appeared at 14, 146 and 148°C for Mn-CeO_x/Ti-PILC(S), Mn-CeO_x/Ti-PILC(O) and Mn-CeO_x/Ti-PILC(Cl) respectively, which were uniformly lower than Mn-CeO_x/clay of 168°C, suggesting that the acidity was weaker for Ti-containing catalysts in comparison with Mn-CeO_x/clay.

It can be seen that the overall acidity of the three cata-

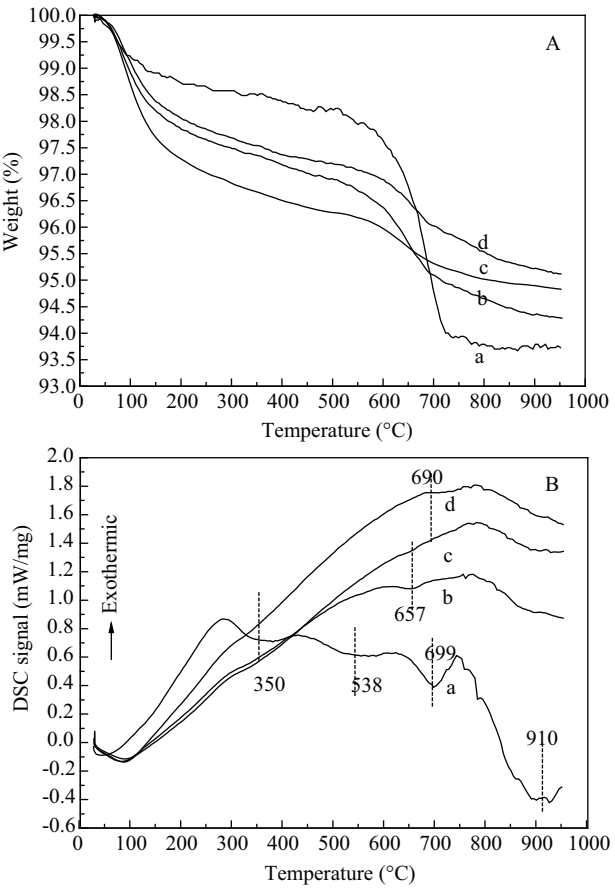

Fig. 3 TG (A) and DSC (B) curves of the samples. Line a: Mn-CeO_x/clay; line b: Mn-CeO_x/Ti-PILC(Cl); line c: Mn-CeO_x/Ti-PILC(O); line d: Mn-CeO_x/Ti-PILC(S).

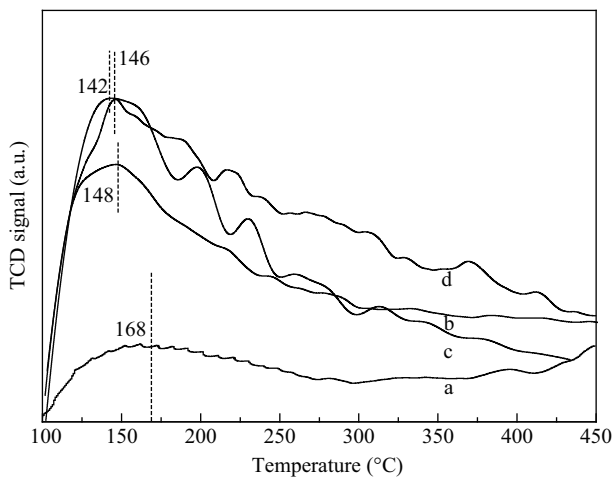

Fig. 4 NH_3-TPD patterns of the samples. Line a: Mn-CeO_x/clay; line b: Mn-CeO_x/Ti-PILC(Cl); line c: Mn-CeO_x/Ti-PILC(O); line d: Mn-CeO_x/Ti-PILC(S).

lysts supported over Ti-PILCs was much larger than that of Mn-CeO_x/clay. The enhancement in acidity arose from the exposure of the layer structure and the introduced pillar metal oxide (Binitha and Sugunan, 2006). For the pillared clays, the acidity and acid site types (Lewis and Bronsted) related with many factors including the preparation method (Bradley and Kydd, 1993; He et al., 1998; Del Castillo et al., 2000). In the case of the catalysts supported over Ti-PILCs prepared with different methods, the order of the overall acidity resulted to be: Mn-CeO_x/Ti-PILC(S) > Mn-CeO_x/Ti-PILC(O) > Mn-CeO_x/Ti-PILC(Cl).

2.1.5 H_2-TPR results

Temperature-programmed reduction has been described as a sensitive technique for studying the reducibility and has been applied successfully for the characterization of catalysts (Jones and Nicol, 1986). The H_2-TPR results are displayed in Fig. 5. H_2-TPR spectra of all the catalyst samples were featured by one peak spread over a wide temperature range (100–600°C). This was similar to the unsupported Mn-CeO_x (Delimaris and Ioannides, 2008). The spanned peak resulted from the reduction process

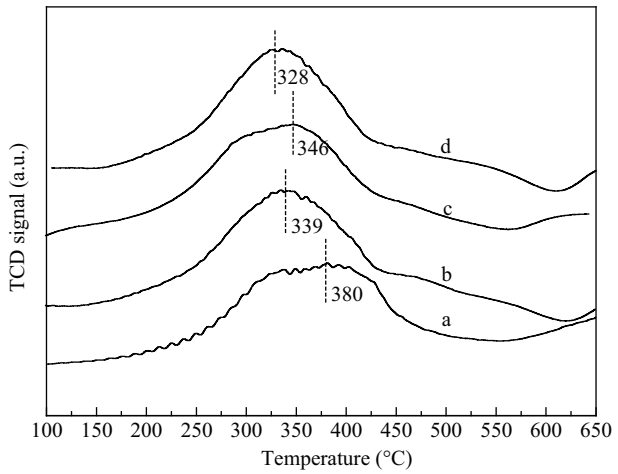

Fig. 5 H_2-TPR patterns of the samples. Line a: Mn-CeO_x/clay; line b: Mn-CeO_x/Ti-PILC(Cl); line c: Mn-CeO_x/Ti-PILC(O); line d: Mn-CeO_x/Ti-PILC(S).

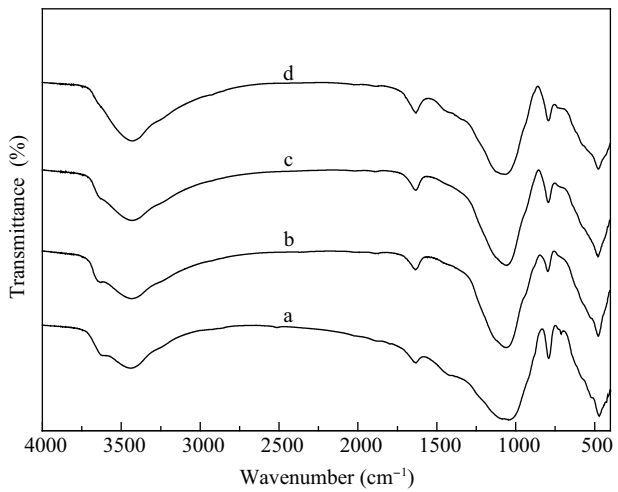

Fig. 6 FT-IR spectra of the samples. Line a: Mn-CeO_x/clay; line b: Mn-CeO_x/Ti-PILC(Cl); line c: Mn-CeO_x/Ti-PILC(O); line d: Mn-CeO_x/Ti-PILC(S).

of manganese and ceria oxides for all the catalysts. But the assignment of the afore mentioned peaks to specific reduction steps was not straight because the reduction of Ce^{4+} to Ce^{3+} took place along with reduction that of manganese ions (Delimaris and Ioannides, 2008). For Mn-CeO_x/clay, the peak maximum located between 300–450°C with the highest peak at 380°C. Nevertheless, the peaks for Mn-CeO_x/Ti-PILCs become more intense and distinct, especially for Mn-CeO_x/Ti-PILC(S) with its relatively intense peak centered at 328°C. A shift in the TPR peaks to lower temperatures seemed to be observed for Mn-CeO_x/Ti-PILCs. The different feature of the peaks and the decrease of the reduction temperatures indicated that the reductions of manganese and cerium oxides were promoted due to the insertion of Ti-pillar to the clay. In this respect, Ettireddy et al. (2006) have also reported there was a strong interaction between the MnO_x and the support TiO_2, which allowed the reduction of manganese oxides at lower temperature.

2.1.6 FT-IR results

Figure 6 shows the FT-IR spectra of the samples. The FT-IR spectrum of Mn-CeO_x/clay exhibited two peaks at 3630 and 3440 cm^{-1} at the –OH stretching region, these two bands were assigned, respectively, to the –OH stretching vibration of the structural hydroxyl groups in the clay and the water molecules present in the interlayer. The band around 1600 cm^{-1} was attributed to the bending vibrations of water. The band at 1060 cm^{-1} was due to asymmetric stretching vibrations of SiO_2 tetrahedral, and a band around 800 cm^{-1} resulted from stretching vibration of Al tetrahedral. The peak at 526–471 cm^{-1} was due to bending vibration of Si–O (Binitha and Sugunan, 2006; Ettireddy et al., 2007). For Ti-PILCs supported catalysts, the broadened bands around 3440 cm^{-1} probably may be due to the introduction of more –OH groups during pillaring process for the Mn-CeO_x/Ti-PILCs in comparison with Mn-CeO_x/clay.

2.2 SCR catalytic activity

As shown in Fig. 7, Ti-PILC(S) displayed low activity, the highest NO conversion was only 15%. The loading of Mn-CeO_x mixed oxides on Ti-PILC resulted in a significant enhancement for NO conversion. More than 80% NO conversion was achieved at 180°C for Mn-CeO_x/Ti-PILC(S). By contrast, the highest NO conversion remained less than 47% for Mn-CeO_x/clay. Accordingly, it might be concluded that Ti-pillar also contributed a lot to the activity of Mn-CeO_x/Ti-PILC though Mn-CeO_x was a decisive factor.

For Mn-CeO_x/Ti-PILCs samples, NO conversions increased with increasing temperature and reached a maximum about 98%, 85% and 83% for Mn-CeO_x/Ti-PILC(S), Mn-CeO_x/Ti-PILC(O) and Mn-CeO_x/Ti-PILC(Cl) respectively. The catalytic activity of Mn-CeO_x/Ti-PILC(S) was distinctly higher than that of Mn-CeO_x/Ti-PILC(Cl) and Mn-CeO_x/Ti-PILC(O). Mn-CeO_x/Ti-PILC(Cl) showed the lowest NO conversion among the three catalysts. The difference in activity for the three catalysts was related

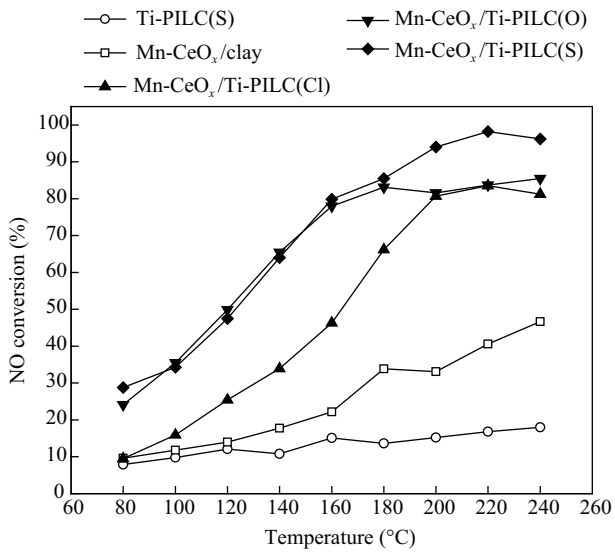

Fig. 7 NO conversions over Ti-PILC(S), Mn-CeO$_x$/clay and Mn-CeO$_x$/Ti-PILCs. Reaction conditions: 0.06 vol.% NO, 0.06 vol.% NH_3, 3 vol.% O_2, balance N_2, GHSV 50.000 hr^{-1}, total flow rate 300 mL/min.

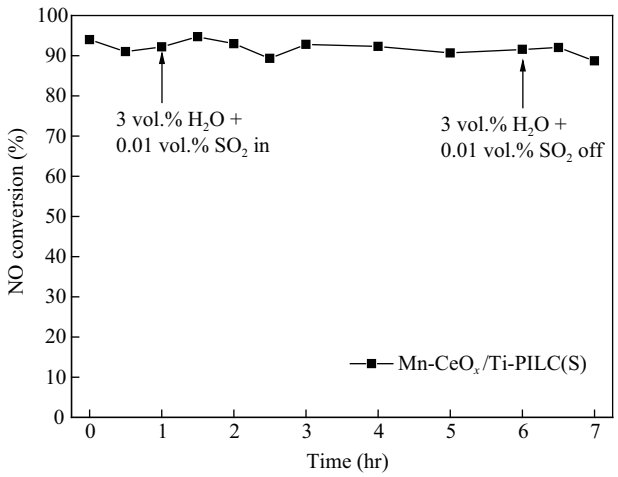

Fig. 8 Effect of H_2O and SO_2 on NO conversion over Mn-CeO$_x$/Ti-PILC(S) at 200°C. Reaction conditions: 0.06 vol.% NO, 0.06 vol.% NH_3, 3 vol.% O_2, 3 vol.% H_2O (when used), 0.01 vol.% SO_2 (when used), balance N_2, GHSV 50,000 hr^{-1}, total flow rate 300 mL/min.

to the reaction temperature, there was little gap between Mn-CeO$_x$/Ti-PILC(S) and Mn-CeO$_x$/Ti-PILC(O) at lower temperature range (80–180°C) while the activity showed great difference at relatively higher temperature range (180–240°C). On the contrary, great gap between Mn-CeO$_x$/Ti-PILC(O) and Mn-CeO$_x$/Ti-PILC(Cl) emerged at lower temperature range (80–180°C).

Because the SCR catalyst is usually deactivated mainly by H_2O and residue SO_2 in the flue gases, the effect of H_2O and SO_2 on Mn-CeO$_x$/Ti-PILC(S) has also been investigated at 200°C. It could be seen from Fig. 8 that Mn-CeO$_x$/Ti-PILC(S) exhibited good resistance to H_2O and SO_2 in the presence of 3 vol.% H_2O and 0.01 vol% SO_2. No obvious decrease in NO conversion was found, and the NO conversion was stable around 90% in 5 hr in the presence of 3 vol.% H_2O and 0.01 vol.% SO_2.

According to the characterization results, it was concluded that effective insertion of Ti-pillar into the clay can obtain the Mn-CeO$_x$/Ti-PILC with lager surface area and pore volume, enhanced surface acidity, higher thermal stability and different redox properties. Among all three Mn-CeO$_x$/Ti-PILCs, Mn-CeO$_x$/Ti-PILC(Cl) suffered a relatively unsuccessful pillaring process, with the smallest surface area, pore volume and the surface acidity. These might be the reason for the lowest catalytic activity for Mn-CeO$_x$/Ti-PILC(Cl). With regard to Mn-CeO$_x$/Ti-PILC(S) with superior activity, it maintained the largest acidity which was beneficial for SCR process (Chio et al., 1996; Zuo et al., 2008), also taking into account its unique structure and textural properties that it preserved the largest pore volume and moderate pore diameter. It has been reported in the previous literature (Gil et al., 2001; Xia et al., 2001) that the structure of PILCs had a marked effect on the activity. Accordingly, it might be deduced that the superior activity of Mn-CeO$_x$/Ti-PILC(S) could be attributed to the pore structure to some degree, the extra-lattice TiO_2 might be another reason, as TiO_2 is a more promising support for MnO_x containing systems including Mn-CeO$_x$ (Smirniotis et al., 2006; Tang et al., 2007; Wu et al., 2008; Yu et al., 2010),

Combining the activity results, it can be seen that the order of the surface area, which decreased as follows: Mn-CeO$_x$/Ti-PILC(O) > Mn-CeO$_x$/Ti-PILC(S) > Mn-CeO$_x$/Ti-PILC(Cl). This was not in exact coherence with that of the activity, suggesting that the surface area was not decisive but favorable for Mn-CeO$_x$/Ti-PILCs, By contrast, the order of the surface acidity concentration Mn-CeO$_x$/Ti-PILC(S) > Mn-CeO$_x$/Ti-PILC(O) > Mn-CeO$_x$/Ti-PILC(Cl), accorded with that of the catalytic activity, it can be concluded that the acidity was an important factor with respect to the SCR activity of Mn-CeO$_x$/Ti-PILCs.

Absorption and activation of NH_3 over acid sites was a key step in Eley-Rideal (E-R) SCR mechanism. The role of absorbed ammonia species over different acid sites (Lewis and Bronsted) was influenced by temperature (Chen et al., 2009, 2010). It was assumed that absorbed ammonia species over Bronsted acid sites were helpful in SCR process at higher temperature range (180–240°C), while Lewis acid was more important at the temperature range 80–180°C. For Mn-CeO$_x$/Ti-PILCs, it was deduced that the distribution of acid sites over three Mn-CeO$_x$/Ti-PILCs was different, Mn-CeO$_x$/Ti-PILC(S) exhibited the largest amounts of both Bronsted and Lewis acid sites, so it exhibited the highest activity in the whole studied temperature window. By contrast, amounts of Bronsted acid sites may be smaller for Mn-CeO$_x$/Ti-PILC(O), resulting in its lower activity at 180–240°C, and lower NO conversions of Mn-CeO$_x$/Ti-PILC(Cl) compared to Mn-CeO$_x$/Ti-PILC(O) at 80–180°C may be due to the smaller amounts of Lewis acid sites.

3 Conclusions

According to the characterization results of these catalysts, it can be concluded that Ti-pillaring could help to increase the specific surface area, pore volume, surface acid and thermal stability for the catalysts. Among all three

Mn-CeO_x/Ti-PILCs, the enhancement for Mn-CeO_x/Ti-PILC(S) and Mn-CeO_x/Ti-PILC(O) was more obvious than Mn-CeO_x/Ti-PILC(Cl).

Pillaring the clay with titanium contributed to the greatly enhanced activity of Mn-CeO_x/Ti-PILC, which exhibited more than 80% for SCR of NO with NH_3 at low temperature. Among three Mn-CeO_x catalysts supported over Ti-PILCs, Mn-CeO_x/Ti-PILC(S) showed the highest SCR activity, and 98% NO conversion was obtained at 220°C, at the same time, Mn-CeO_x/Ti-PILC(S) exhibited good resistance to SO_2 and H_2O.

Acknowledgments

This work was supported by the National Natural Science Foundation of China (No. 50976050, 51176077), and the Research Fund for International Young Scientists (NO. 51150110155).

References

Auerbach S M, Carrado K A, Dutta P K, 2004. Handbook of Layered Materials. Marcel Dekker, New York.

Binitha N N, Sugunan S, 2006. Preparation, characterization and catalytic activity of titania pillared montmorillonite clays. *Microporous and Mesoporous Materials*, 93(1-3): 82–89.

Boudali L K, Ghorbel A, Grange P, 2006. SCR of NO by NH_3 over V_2O_5 supported sulfated Ti-pillared clay: Reactivity and reducibility of catalysts. A*pplied Catalysis A: General*, 305(1): 7–14.

Bradley S M, Kydd R A, 1993. A comparison of the catalytic activities of Ga_{13}^-, Al_{13}^-, $GaAl_{12}^-$ and chromium-pillar interlayered clay minerals and Ga-H-ZSM-5 zeolite in the dehydrocyclodimerization of propane. *Journal of Catalysi*s, 142(2): 448–454.

Carja G, Kameshima Y, Okada K, Madhusoodana C D, 2007. Mn-Ce/ZSM-5 as a new superior catalyst for NO reduction with NH_3. *Applied Catalysis B: Environmental*, 73(1-2): 60–64.

Casapu M, Krocher O, Elsener M, 2009. Screening of doped MnO_x-CeO_2 catalysts for low-temperature NO-SCR. *Applied Catalysis B: Environmental*, 88(3-4): 413–419.

Chae H J, Nam I S, Ham S W, Hong S B, 2004. Characteristics of vanadia on the surface of V_2O_5/Ti-PILC catalyst for the reduction of NO_x by NH_3. *Applied Catalysis B: Environmental*, 54(2): 117–126.

Chen L, Li J H, Ge M F, 2009. Promoting effect of Ce-doped V_2O_5-WO_3/TiO_2 with low vanadium loadings for selective catalytic reduction of NO_x by NH_3. *Journal of Physical and Chemical C*, 113(50): 21177–21184.

Chen L, Li J H, Ge M F, 2010. DRIFT study on cerium-tungsten/titania catalyst for selective catalytic reduction of NO_x with NH_3. *Environmental Science and Technology*, 44(24): 9590–9596.

Chmielarz L, Kuśtrowski P, Zbroja M, Rafalska-Lasocha A, Dudek B, Dziembaj R, 2003. SCR of NO by NH_3 on alumina or titania-pillared montmorillonite various modified with Cu or Co: Part I. General characterization and catalysts screening. *Applied Catalysis B: Environmental*, 45(2): 103–116.

Choi E Y, Nam I S, Kim Y G, 1996. TPD study of mordenite-type zeolites for selective catalytic reduction of NO by NH_3. *Journal of Catalysis*, 161(2): 597–604.

Cool P, Zhu H Y, Cassiers K, Vansant E F, 2004. Novel strategies towards mesoporous titania and titania-silicate composites. *Studies Surface Science Catalysis*, 154: 789–796.

Del Castillo H L, Gil A, Grange P, 2000. Preparation and characterization of sulfated titanium-modified pillared montmorillonite. *Catalysis Letters*, 43(1-2): 133–137.

Delimaris D, Ioannides T, 2008. VOC oxidation over MnO_x-CeO_2 catalysts prepared by a combustion method. *Applied Catalysis B: Environmental*, 84(1-2): 303–312.

Ettireddy P R, Ettireddy N, Mamedov S, Boolchand P, Smirniotis P G, 2007. Surface characterization studies of TiO_2 supported manganese oxide catalysts for low temperature SCR of NO with NH_3. *Applied Catalysis B: Environmental*, 76(1-2): 123–134.

García-Cortés J M, Pérez-Ramírez J, Illán-Gómez M J, Kapteijn F, Moulijn J A, de Lecea C S M, 2001. Comparative study of Pt-based catalysts on different supports in the low-temperature de-NO_x-SCR with propene. *Applied Catalysis B: Environmental*, 30(3-4): 399–408.

Gil A, Vicente M A, Lambert J F, Gandía, L M, 2001. Platinum catalysts supported on Al-pillared clays: Application to the catalytic combustion of acetone and methyl-ethyl-ketone. *Catalysis Today*, 68(1-3): 41–51.

Gregg S J, Sing K S W, 1982. Adsorption, Surface Area and Porosity (2nd ed). Academic Press, New York.

He M Y, Liu Z H, Min E Z, 1988. Acidic and hydrocarbon catalytic properties of pillared clay. *Catalysis Today*, 2(2-3): 321–338.

Jones A, MicNicol B M, 1986. Temperature-Programmed Reduction for Solids Materials Characterization. Marcel Dekker, New York.

Linda S C, Yang R T, Chen N, 1996. Iron oxide and chromia supported on titania-pillared clay for selective catalytic reduction of nitric oxide with ammonia. *Journal of Catalysis*, 164(1): 7–81.

Li J H, Chen J J, Ke R, Luo C K, Hao J M, 2007. Effects of precursors on the surface Mn species and the activities for NO reduction over MnO_x/TiO_2 catalysts. *Catalysis Communications*, 8(12): 1896–1900.

Long R Q, Yang R T, 1999. Selective catalytic reduction of nitrogen oxides by ammonia over Fe^{3+}-exchanged TiO_2-pillared clay catalysts. *Journal of Catalysis*, 186(2): 254–268.

Long R Q, Yang R T, 2000a. Selective catalytic reduction of NO with ammonia over V_2O_5 doped TiO_2 pillared clay catalysts. *Applied Catalysis B: Environmental*, 24(1): 13–21.

Long R Q, Yang R T, 2000b. The promoting role of rare earth oxides on Fe-exchanged TiO_2-pillared clay for selective catalytic reduction of nitric oxide by ammonia. *Appllied Catalysis B: Environmental*, 27(2): 87–95.

Qi G S, Yang R T, Chang R, 2004. MnO_x-CeO_2 mixed oxides prepared by co-precipitation for selective catalytic reduction of NO with NH_3 at low temperatures. *Applied Catalysis B: Environmental*, 51(2): 93–106.

Romero A, Dorado F, Asencio I, García P B, Valverde J L, 2006. Ti-Pillared clays: synthesis and general characterization. *Clays and Clay Minerals*, 54(6): 737–747.

Sing K S W, Everett D H, Haul R A W, Moscou L, Pierotti R A, Rouquérol J et al., 1985. Physical and biophysical chemistry division commission on colloid and surface chemistry including catalysis. *Pure and Applied Chemistry*, 57(4): 603–619.

Smirniotis P G, Sreekanth P M, Pena D A, Jenkins R G, 2006.

Manganese oxide catalysts supported on TiO_2, Al_2O_3, and SiO_2: A comparison for low-temperature SCR of NO with NH_3. *Industrial and Engineering Chemistry Research*, 45(19): 6436–6443.

Tang X L, Hao J M, Yi H H, Li J H, 2007. Low-temperature SCR of NO with NH_3 over AC/C supported manganese-based monolithic catalysts. *Catalysis Today*, 126(3-4): 406–411.

Wu Z B, Jin R B, Liu Y, Wang H Q, 2008. Ceria modified MnO_x/TiO_2 as a superior catalyst for NO reduction with NH_3 at low-temperature. *Catalysis Communications*, 9(13): 2217–2220.

Wu Z B, Jin R B, Liu Y, Wang H Q, 2009, Effect of ceria doping on SO_2 resistance of Mn/TiO_2 for selective catalytic reduction of NO with NH_3 at low temperature. *Catalysis Communications*, 10(6): 935–939.

Xia Q H, Hidajat K, Kawi S, 2001. Adsorption and catalytic combustion of aromatics on platinum-supported MCM-41 materials. *Catalysis Today*, 68(1-3): 255–262.

Yang R T, Chen J P, Kikkinides E S, Cheng L S, Cichanowicz J E, 1992. Pillared clays as superior catalysts for selective catalytic reduction of NO with NH_3. *Industrial and Engineering Chemistry Research*, 31(6): 1440–1445.

Yang R T, Li W B, 1995. Ion-exchanged pillared clays: A new class of catalysts for selective catalytic reduction of NO by hydrocarbons and by ammonia. *Journal of catalysis*, 154(2): 414–417.

Yu D Q, Liu Y, Wu Z B, 2010. Low-temperature catalytic oxidation of toluene over mesoporous MnO_x-CeO_2/TiO_2 prepared by sol-gel method. *Catalysis Communications*, 11(8): 788–791.

Yuan P, He H P, Bergaya F, Wu D Q, Zhou Q, Zhu J X, 2006. Synthesis and characterization of delaminated iron-pillared clay with meso-microporous structure. *Microporous and Mesoporous Materials*, 88(1-3): 8–15.

Zuo S F, Huang Q Q, Zhou R X, 2008. Al/Ce pillared clays with high surface area and large pore: Synthesis, characterization and supported palladium catalysts for deep oxidation of benzene. *Catalysis Today*, 139(1-2): 88–93.